Permeability Control of Glucose-Sensitive Nanoshells

Yongjun Zhang,[†,‡] Ying Guan,[†,‡] and Shuiqin Zhou[*,†]

Department of Chemistry of College of Staten Island, and The Graduate Center, The City University of New York, 2800 Victory Boulevard, Staten Island, New York 10314, and Institute of Polymer Chemistry, Nankai University, Tianjin 300071, China

To study the permeability of hydrogel in nanoscale thickness, core–shell microgels with degradable poly(*N*-isopropylacrylamide) (PNIPAM) as the core and nondegradable phenylboronic acid (PBA)-conjugated poly(*N*-isopropylacrylamide) [P(NIPAM-PBA)] as the shell were designed and synthesized. Laser light scattering was used to study the volume phase transitions and core degradation behavior of the core–shell microgels. The release of the degraded core polymer chains can be conveniently followed by turbidity change. At room temperature, the degraded polymer segments diffuse freely out of the precursor poly(*N*-isopropylacrylamide-co-acrylic acid) gel shells in water. In contrast, the PBA-modified P(NIPAM-PBA) nanoshell can hold most of the degraded core polymer chains under the same conditions, thanks to its condensed structure at the collapsed state. Lowering the temperature or increasing pH increases the swelling degree of the P(NIPAM-PBA) shell, which provides methods to control its permeability by temperature and pH. The complexation of PBA groups with glucose also enhances the swelling of the nanoshell and, thus, increases its permeability. The understanding of how to control the permeability of the glucose-sensitive gel nanoshell in hollow microgel particles is very important for further design of self-regulated insulin delivery systems.

Introduction

Hydrogels are cross-linked polymeric networks that absorb and retain a large amount of water. Microgels are gel particle dispersions with average diameters ranging between 50 nm and 5 mm.[1] Because of their small size, microgels exhibit rapid swelling or shrinking in response to environmental changes. They have been used as model colloids for the theoretical study of soft matters.[2] They have also found applications in a wide range of areas,[3] such as sensing,[4] separation, purification,[5] microreactor for the synthesis of nanoparticles,[6,7] and the fabrication of photonic crystals.[8,9]

Colloidal microgels are particularly suitable for application as controlled drug delivery systems.[10] The drugs can be incorporated and then released from the microgel interior due to the open network of the microgel structure. The rapid response of microgels to various environmental stimuli, such as pH, temperature, and ionic strength, can be exploited to trigger the release of drugs.[11,12] Furthermore, the small size of microgels makes the simple administration via injection possible. In addition, the easy functionalization of microgels allows one to modify the microgel surface by attaching receptor-specific ligands to gain targeting ability to specific sites.[13,14]

Control over the permeability of certain drugs from the interior to the outside of microgels is the key for their application as controlled drug delivery systems. Although there have been extensive studies on various microgel designs and trigger mechanisms, the study of the permeability of microgels is difficult, mainly because of their small size. Moore et al. studied ion penetration through a fatty acid coating barrier into microgel with a relatively large size (400 μm in diameter).[15] Recently, Lyon et al.[16] manipulated the pore size of the shell of a core–shell microgel through the cleavage of the cross-links in the shell. The resulting shell will only allow proteins with a size smaller than the pore to pass through.

To develop a self-regulated insulin delivery system, we have synthesized monodispersed glucose-sensitive poly(*N*-isopropylacrylamide) microgels using the phenylboronic acid group as the glucose-responsive moiety.[17] Their thermosensitive and glucose-sensitive behaviors were studied using a light scattering technique in terms of size change. In the presence of glucose, a dramatic increase in particle size was observed due to the glucose-induced swelling of the microgel. Several different research groups have also investigated the volume phase transitions of the PNIPAM-based glucose responsive microgels in detail at the same time.[18–20] In this work, we designed and synthesized a series of core–shell structured microgels with a degradable core. The cross-links in the core can be destroyed and the release of the degraded polymer debris inside the core through the shell can be traced conveniently by turbidity change. Our results show that the permeability of the glucose-sensitive gel nanoshell can be controlled through the change in temperature, pH, and glucose concentration under different experimental conditions, which provides an important basis for further development of self-regulated insulin delivery system.

Experimental Section

Materials. *N*-Isopropylacrylamide (NIPAM), *N,N*′-methylenebis-(acrylamide) (BIS), *N,N*′-(1,2-dihydroxyethylene)bisacrylamide (DHEA), ammonium persulfate (APS), sodium dodecyl sulfate (SDS), acrylic acid (AA), and *N*-(3-dimethylaminopropyl)-*N*′-ethyl-carbodiimide hydrochloride (EDC) are all purchased from Aldrich. 3-Aminophenylboronic acid (APBA) and D-(+)-glucose were purchased from Acros. NIPAM was purified by recrystallization from a hexane/acetone mixture and dried in vacuum. AA was distilled under reduced pressure. Other reagents were used as received.

Microgel Synthesis. A series of core–shell microgels from the same core solution but with different shell thicknesses were synthesized. The

* To whom correspondence should be addressed. Email: zhoush@mail.csi.cuny.edu.
† The City University of New York.
‡ Nankai University.

Table 1. Recipe for the Synthesis of Core–Shell Microgels with Different Shell Thicknesses

|	core solution	water	SDS solution	shell solution	0.06 M APS
CSM1	25 mL	58.75 mL	10 mL	6.25 mL	5 mL
CSM2	25 mL	52.5 mL	10 mL	12.5 mL	5 mL
CSM3	25 mL	40 mL	10 mL	25 mL	5 mL

Scheme 1. Modification of the P(NIPAM-AA) Shell with 3-Aminophenylboronic Acid (APBA)
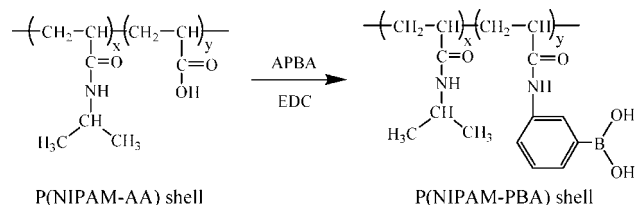
core was cross-linked with the degradable cross-linker DHEA, while the shell was cross-linked with the nondegradable cross-linker BIS. To synthesize the core microgel, 1.4 g of NIPAM, 0.28 g of DHEA, and 0.088 g of SDS were dissolved in 50 mL of water. The solution was filtered and transferred to a 250 mL three-necked flask with the help of 150 mL of water. The mixture was purged with N_2 and heated to 70 °C. After 1 h, 5 mL of 0.06 M APS was added to initiate the polymerization. The reaction was allowed to proceed for 5 h. The resultant microgel was dialyzed against water for 1 week to remove impurities.

A stock shell solution was prepared by dissolving 1.4 g of NIPAM, 0.03 g of BIS, and 0.113 g of AA in 100 mL of water. A stock SDS solution was prepared by dissolving 0.57 g of SDS in 100 mL of water. To synthesize core–shell microgels with different shell thicknesses, the core solution, SDS solution, and water, according to the recipe in Table 1, were added to a flask. The mixture was purged with N_2 and heated to 70 °C for 1 h before the preheated shell solution was added. The mixture was purged with N_2 for another 30 min, followed by adding 5 mL of 0.06 M APS to initiate the polymerization. The reaction was allowed to proceed for 5 h. The resultant microgels were dialyzed against water for 1 week to remove impurities. The DHEA-cross-linked PNIPAM core/BIS-cross-linked P(NIPAM-AA) shell microgels were denoted as CSM1, CSM2, and CSM3, respectively. According to the different amount of shell solution fed, the microgels have a shell thickness increase in the order of CSM1 < CSM2 < CSM3.

Shell Modification with 3-Aminophenylboronic Acid (APBA). To 50 mL of the core–shell microgels, which was cooled with an ice–water bath, 0.233 g of APBA (0.025 M) and 0.239 g of EDC (0.025 M) were added. The reaction mixture was kept at about 0 °C for 2 h. The resultant products were purified by dialysis against water. The resultant DHEA-cross-linked PNIPAM core/BIS-cross-linked P(NIPAM-PBA) shell microgels were denoted as CSBM1, CSBM2, and CSBM3, respectively. The conjugation of PBA groups to the shell was shown in Scheme 1.

Dynamic Laser Light Scattering (LLS). A standard LLS spectrometer (BI-200SM) equipped with a BI-9000 AT digital time correlator (Brookhaven Instrument, Inc.) was used to monitor the size and size distribution of the microgels under different conditions. A He-Ne laser (35 mW, 633 nm) was used as the light source. The solutions were passed through 0.45 μm Millipore Millex-HV filters to remove dust. In dynamic LLS, the Laplace inversion of each measured intensity–intensity time correlated function can result in a characteristic line width distribution G(Γ).[21] For a purely diffusive relaxation, Γ is related to the translational diffusion coefficient D by $(\Gamma/q^2)_{C\to 0, q\to 0} = D$, where $q = (4\pi n/\lambda)\sin(\theta/2)$, with n, λ, and θ being the solvent refractive index, the wavelength of the incident light in vacuum, and the scattering angle, respectively. G(D) can be further converted to a hydrodynamic radius (R_h) distribution by using the Stokes–Einstein equation, $R_h = (k_B T/6\pi\eta)D^{-1}$, where T, k_B, and η are the absolute
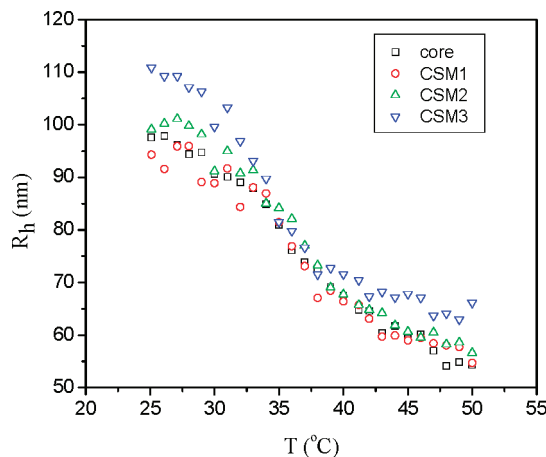
Figure 1. Average R_h value of the PNIPAM core/P(NIPAM-AA) shell microgels as a function of temperature, measured at pH = 3.5 and a scattering angle $\theta = 90°$.

temperature, the Boltzmann constant, and the solvent viscosity, respectively.[22]

Turbidity Measurement. The turbidity is represented by the absorbance at 600 nm. Measurement was carried out on a Perkin-Elmer Lambda 650 spectrophotometer. The temperature of the sample was controlled by a circulation–water bath (Fisher Scientific).

Results and Discussion

Synthesis of the Core–Shell Microgels. The core–shell microgels, with a DHEA-cross-linked PNIPAM core and a BIS-cross-linked P(NIPAM-AA) shell were synthesized using the method first developed by Lyon et al.[23] The core–shell microgels (CSM1–3) have the same core but different shell thicknesses. Figure 1 shows the temperature dependence of the particle size of the core–shell microgels measured at pH = 3.5. According to the amount of shell solution fed, the core–shell microgels are expected to have a shell thickness increase in the order of parent core microgel < CSM1 < CSM2 < CSM3. However, only CSM3 was found to be larger than the parent core at both swollen and collapsed states. CSM2 is larger than the parent core at the swollen state, but little difference was found at the collapsed state. For CSM1, its size is very close to that of the parent core at both states, indicating a very thin shell was added. For CSM3 with the thickest shell, the P(NIPAM-AA) shell thickness is about 13 and 8 nm at swollen (25 °C) and collapsed (45 °C) states, respectively. It was known that the swelling behavior of a core–shell microgel is not a simple addition of the individual core and shell components. The mutual interaction between the shell and the core has been studied in detail.[24,25] However, at pH = 3.5, the PNIPAM core/P(NIPAM-AA) shell microgels and the parent PNIPAM core microgel present a similar thermosensitive behavior with a single volume phase transition temperature (VPTT) of about 32 °C, indicating that the addition of a P(NIPAM-AA) shell does not significantly change the VPTT of the microgels. This result is in agreement with the observation of Lyon et al. under similar conditions.[23] The phase transition curves of the microgels are broad because of the high cross-link density (10 mol% DHEA) in the core.

The phenylboronic acid group was introduced by amidation of the carboxylic acid groups with 3-aminophenylboronic acids to make the shell glucose-responsive. Figure 2 shows the thermosensitive behaviors of the resulting core–shell microgels CSBM1–3 at pH = 3.5 and a comparison with that of the parent core. For all three core–shell microgels, two distinct volume
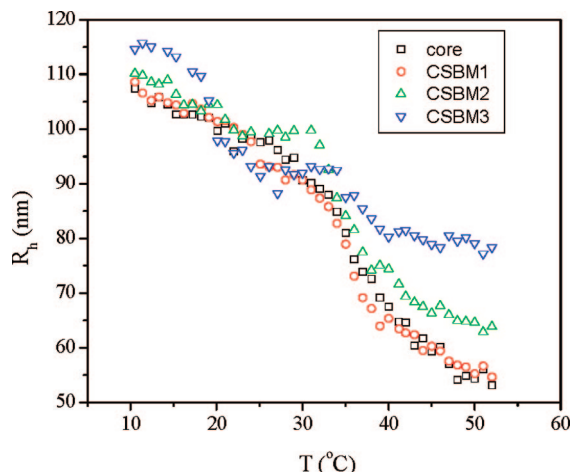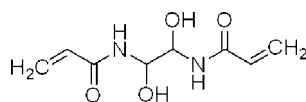
Figure 2. Average R_h value of the PNIPAM core/P(NIPAM-PBA) shell microgels as a function of temperature, measured at pH = 3.5 and a scattering angle $\theta = 90°$.

Scheme 2. Structure of the Degradable Cross-Linker DHEA

Figure 3. Absorbance change of the DHEA-cross-linked PNIPAM core/BIS-cross-linked P(NIPAM-AA) shell microgels CSM1–3 and the parent DHEA-cross-linked PNIPAM core microgel upon addition of NaIO$_4$ in water, with a final NaIO$_4$ concentration of 0.05 M, measured at $\lambda = 600$ nm and $T = 25$ °C.

phase transitions were observed. Such clear two-stage deswelling behavior has been previously reported in doubly thermosensitive core–shell microgels.[26,27] The phase transition around 34 °C can be assigned to the one induced from the PNIPAM core, while the phase transitions at the lower temperatures of 24, 20, and 18 °C can be assigned to those of the P(NIPAM-PBA) shell for CSBM1, CSBM2, and CSBM3, respectively. We have reported that the replacement of the carboxylic acid groups in the P(NIPAM-AA) microgel (10 mol% AA) by the hydrophobic PBA groups significantly reduced its VPTT from about 32 °C to about 17 °C at pH = 3.5.[17] The P(NIPAM-PBA) shells in the core–shell microgels of CSBM1–3 have the same chemical composition and should present a similar VPTT at the same pH value. Apparently the presence of the PNIPAM core shifts the VPTT of the P(NIPAM-PBA) gel shell to a higher temperature. The collapse of the shell is retarded because of the restriction of the core. Only at a higher temperature can the effect of the core be overcome and a decrease in particle size be observed. The results presented in Figure 2 also indicate that the core effect on the VPTT of the shell is more significant for a thin shell. For the thinnest shell in CSBM1, its VPTT increased by 7 °C due to the core restriction, while only a 1 °C increase in VPTT was observed for the thickest shell of CSBM3. It is reasonable that the ability of the shell to overcome the core restriction increases with its thickness. Although the effect of a shell on the thermosensitive swelling behavior of a core have been studied in detail in a core–shell microgel,[23,24] to the best of our knowledge, this is the first observation on how a core may affect the swelling behavior of a shell in a core–shell microgel. We also noticed that the core swelling is compressed by the shell, which is revealed by the decreased size of the CSBM1 and CSBM3 in the temperature range around 20 to 30 °C as compared to the parent core. Specifically, in this intermediate region between phase transition temperatures of shell and core, the collapsed shell can restrict the full swelling of the core. In case of CSBM1, the shell is very thin. The added shell thickness can be smaller than the decrease in core swelling caused by the restriction of collapsed shell. In the case of CSBM3, with the thickest shell, the intense shell restriction can
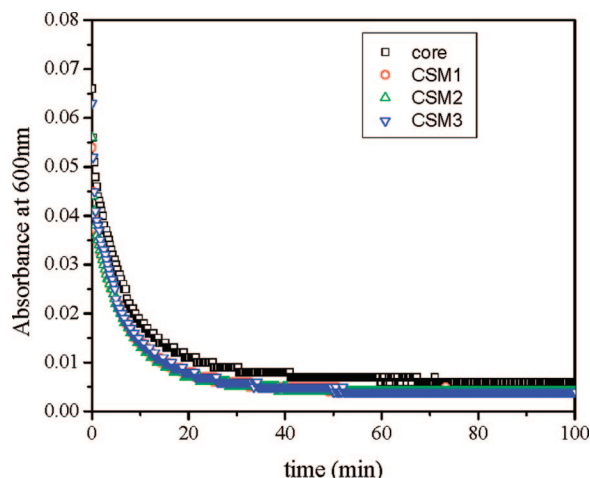
induce a large decrease in core swelling. In such a case, the collapsed shell thickness may not be large enough to compensate the decrease in core swelling due to the shell restriction. Therefore, the overall R_h of both CSBM1 and CSBM3 core–shell particles can be smaller than that of the parent core in this specific temperature range. In the case of CSBM2, with moderate shell thickness, the core swelling is restricted to a certain degree. The added shell thickness might be larger than the decreased core swelling, thus, the overall core–shell particle size exceeds that of the core.

Degradation of the DHEA-Cross-Linked Core. Scheme 2 shows the structure of the degradable cross-linker DHEA used in the core. Its vicinal diol functionality can be cleaved by addition of stoichiometric amount of NaIO$_4$.[28] To synthesize a hollow thermoresponsive microgel, Lyon et al.[29] synthesized a core–shell PNIPAM microgel in which the core is DHEA-cross-linked and the shell is BIS-cross-linked. The addition of NaIO$_4$ degraded the core and the polymer segments diffused out. They found that the turbidity of the microgel suspensions decreases upon the addition of NaIO$_4$ because the linear PNIPAM chains scatter less light compared with the cross-linked microgel. The DHEA-cross-linked PNIPAM core of our core–shell microgels synthesized here can also be degraded in the same way. To achieve this, a final NaIO$_4$ concentration of 0.05 M was used, which is much higher than that of the DHEA cross-links. Importantly, the change in the turbidity of the reaction mixtures provides a convenient way to monitor the core degradation and the diffusion of the degraded polymer chains.

Figure 3 shows the core degradation of the DHEA-cross-linked PNIPAM core/BIS-cross-linked P(NIPAM-AA) shell microgels CSM1–3 in deionized water. For comparison, the degradation of the parent core microgel was also presented. Upon the addition of NaIO$_4$, the absorbances at 600 nm of the microgel suspensions all drop rapidly. The absorbance levels out in about 20 min. Two conclusions can be drawn from these results: (1) the cleavage of the DHEA cross-links in the core is fast and completes in about 20 min; and (2) the addition of a P(NIPAM-AA) shell on the PNIPAM core has no effect on the cleavage of the DHEA cross-links in the core. At 25 °C, the P(NIPAM-AA) shell is in a highly swollen state. The mesh size of the shell is big enough not only for NaIO$_4$ to diffuse freely into the core area, but also for the degradation product to diffuse
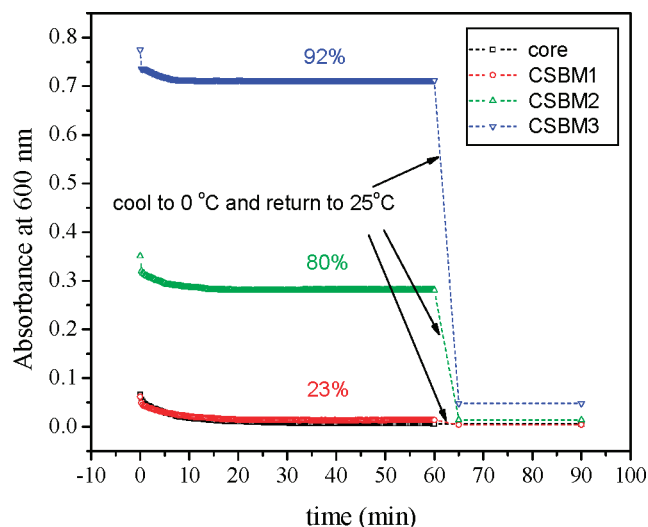
Figure 4. Absorbance change of the DHEA-cross-linked PNIPAM core/BIS-cross-linked P(NIPAM-PBA) shell microgels CSBM1–3 and the parent DHEA-cross-linked PNIPAM core microgel upon addition of NaIO$_4$, with a final concentration of 0.05 M, measured at λ = 600 nm and T = 25 °C. The dash line represents that the samples were cooled to 0 °C and then brought back to 25 °C.

freely out of the core area, therefore, the shell thickness has no effect on their diffusion.

It should be noted that the starting absorbencies are very small for the core and all the CSM1–3 microgels in Figure 3 because both their core and their shells are in a swollen state. In such a case, the difference in the refractive index between the highly swollen microgel particles and the water media is very small. After the modification of the AA groups in the swollen P(NIPAM-AA) shells with the hydrophobic PBA groups, the resultant P(NIPAM-PBA) shells in CSBM1–3 particles are in a collapsed state at 25 °C in water. The shrunk shells have a refractive index much higher than that of the water media. As a result, the ability to scatter light increases with the increase in the P(NIPAM-PBA) shell thickness. As shown in Figure 4, the starting absorbencies increase significantly in the order of CSBM1 < CSBM2 < CSBM3. In the case of CSBM1, the P(NIPAM-PBA) shell is very thin, so the absorbance difference between the CSBM1 and the core is small.

Figure 4 also indicates that the PBA-modified microgels CSBM1–3 have a different absorbance change upon addition of NaIO$_4$. The absorbance of the microgel suspension drops and levels out within 20 min, indicating that NaIO$_4$ can diffuse into the core freely and break the DHEA cross-links. In contrast to the core–shell microgels CSM1–3 without PBA-modification in the shell, the remaining absorbance of the microgels with PBA-modified shell are prominent. For CSBM3 with the thickest shell, the remaining absorbance is 92% of its original absorbance, while for CSBM2 and CSBM1, the remaining absorbances were 80% and 23%, respectively. The result clearly shows that the polymer debris as a result of the degradation of the core by NaIO$_4$ can be held by the P(NIPAM-PBA) shell. At 25 °C, the P(NIPAM-PBA) shell is in a collapsed state and has a very small mesh size that does not allow the degraded polymer segments to diffuse out freely. However, because the PNIPAM core becomes polymer solution upon degradation, an osmotic pressure is built up in the core. As a result, some short polymer segments may leak out. The results shown in Figure 4 indicate that the amount of polymer segments leaked out increases with the decrease in the shell thickness. In another word, the thicker shell can withstand more osmotic pressure and hold more polymer segments.
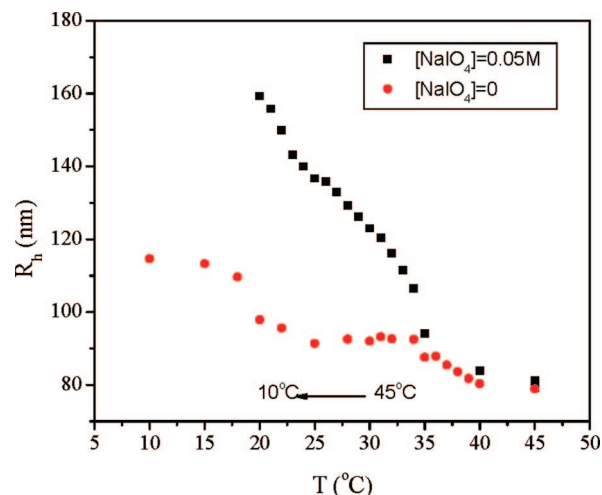

Figure 5. Particle size change of the CSBM3 microgel from 45 to 10 °C in the presence and absence of NaIO$_4$, respectively.
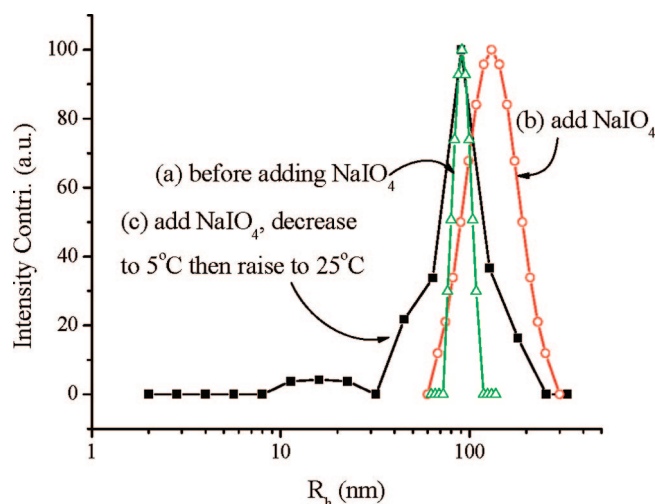

Figure 6. Size distributions of the CSBM3 microgels at T = 25 °C: (a) before NaIO$_4$ treatment, (b) after NaIO$_4$ treatment, and (c) after NaIO$_4$ treatment, the sample was then cooled to 5 °C and brought back to 25 °C.

Controlled Permeability of the P(NIPAM-PBA) Shell. One may expect that the permeability of the P(NIPAM-PBA) shell can be controlled by temperature. To verify it, the NaIO$_4$-treated CSBM1–3 samples were cooled with ice–water to swell the shell. They were then brought back to 25 °C to collapse the shell and the absorbance was measured again. As shown in Figure 4, a decrease in absorbance was observed for all three microgels with a PBA-modified shell after the cooling treatment. The remaining absorbances were 28, 5, and 7% of that before the cooling treatment for CSBM1, CSBM2, and CSBM3, respectively. As a control, the NaIO$_4$-treated core microgel was also cooled with ice–water and brought back to 25 °C, but no change was observed in its absorbance. These results clearly show that the degraded polymer segments held by the P(NIPAM-PBA) shell were released upon cooling because the P(NIPAM-PBA) shell swells at 0 °C and the mesh size of the shell is large enough for the polymer segments to diffuse out of the core area.

The temperature-controlled release of the degradation product was also monitored in situ using dynamic light scattering. A CSBM3 sample was treated with NaIO$_4$ at 45 °C overnight to make sure that the core cross-links were degraded completely. The change in particle size was then followed when the sample was

Scheme 3. Equilibrium of the Phenylboronic Acid Group among an Uncharged Trigonal Form, a Charged Boronate Anion, and the Phenylboronic Acid–Glucose Complex
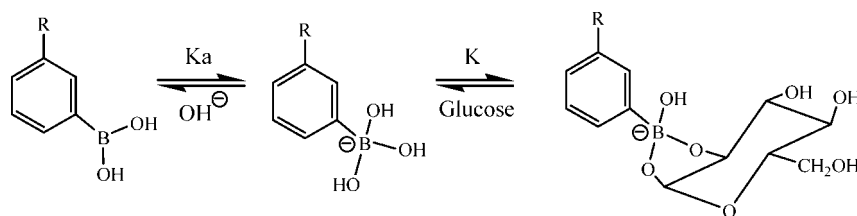

was cooled down from 45 to 10 °C. As a control, the size change of another CSBM3 sample in the absence of NaIO$_4$ was also measured. As shown in Figure 5, in the absence of NaIO$_4$, the CSBM3 microgel presents a reversible two-step thermosensitive volume phase transition that is similar to the curve observed in Figure 2. For example, two transition temperatures around 18 and 34 °C were observed for the shell and core, respectively. Compared with the control, the microgel in the presence of NaIO$_4$ has a larger size. The enlargement of the microgel should be attributed to two factors. On the one hand, the degradation of the core eliminates its restriction on the shell and allows the shell to swell to a larger degree. On the other hand, the osmotic pressure produced by the degraded polymer segments forces the shell to expand. At $T > 34$ °C, the PNIPAM segments in the core area are in a collapsed state. They should only produce a very small osmotic pressure. As a result, the degree of the shell expansion is limited. As the temperature decreases to the one below the VPTT of PNIPAM, the PNIPAM segments become hydrophilic and well dissolved in water. They produce a high osmotic pressure against the shell. As a result, the shell is blown up and presents a much bigger size than the control at the same temperature. As the temperature continues to decrease to below the VPTT of shell, the shell itself begins to swell and the degradation product begins to leak out. We anticipate that the shell size will reduce to close to that of the control particles at the same temperature because there is no osmotic pressure after the release of the polymer segments. Unfortunately, at low temperatures, the coexistence of the released polymer segments with a broad size distribution interferes with the accurate measurement of the hollow shell particle size.

Figure 6 shows the size and size distributions of the CSBM3 microgels before and after NaIO$_4$ treatments, measured at 25 °C. The R_h of the CSBM3 microgels is about 91 nm, and the size distribution is very narrow, which is in accordance with our previous results. NaIO$_4$ was then added to the CSBM3 sample, with a final concentration of 0.05 M. After standing for 2 h to make sure the complete degradation of the core occurred, we measured the size and size distribution again. A larger R_h of 131 nm is obtained due to the osmotic pressure generated by the degradation product and the elimination of core restriction. The size distribution also becomes broader, possibly due to the interference of the measurement by some leaked small polymer segments. The sample was then cooled to 5 °C and brought back to 25 °C. Its size and size distribution were measured again. As shown in Figure 6, a bimodal distribution was observed, in which the larger species can be assigned to the hollow P(NIPAM-PBA) shell particles, which is centered nearly the same size as the original CSBM3 microgel. The smaller species with a broad size distribution can be considered as the released PNIPAM segments from the core degradation. The results clearly show that, at room temperature, the degraded core polymer chains can be held by the P(NIPAM-PBA) shell and released at low temperatures.

The permeability of the P(NIPAM-PBA) shell can also be controlled by pH. As a Lewis acid, the PBA group can exist as an uncharged trigonal form and a charged boronate anion with a $pK_a = 8.2$[30] (Scheme 3). With an increase in pH, more PBA groups will convert from the hydrophobic uncharged form to the hydrophilic charged form. As a result, the swelling degree of the P(NIPAM-PBA) shell will increase along with its permeability. To study the pH effect on the shell permeability, a core-degraded CSBM3 sample was prepared by first treating the microgel with 0.05 M NaIO$_4$ for 1 h, followed by dialyzing against water for 2 days to remove NaIO$_4$. The temperature of the sample was kept at 25 °C during the procedure. The core-degraded sample was mixed with PBS buffers of various pH values at 28 °C, and the turbidity of the mixture was followed spectrometrically. As shown in Figure 7, at pH = 4, the amount of leaked core material is negligible. However, at pH = 5 and 6, a significant decrease in absorbance was observed, indicating a considerable amount of core material leaked out. This result implies that even a small amount of charge formed in the shell can increase the shell permeability significantly. A dramatic decrease in absorbance (by about 66%) was observed at pH = 7, indicating that a large amount of degradation product leaked out. The permeability of the shell continues to increase as pH continues to increase. The results shown in Figure 7 also indicate that the response of the shell toward pH change is very quick. Upon the mixing with the PBS buffer of pH = 9, nearly all of the core materials held by the shell were released in 10 s. Obviously, the rapid response speed should be attributed to the thinness of the gel nanoshell.

It was known that the charged form of the PBA group might be stabilized by complexation with glucose, as shown in Scheme 3. In other words, the presence of glucose may increase the swelling degree of the P(NIPAM-PBA) shell and, thus, its permeability. The effect of glucose on the shell permeability was studied by mixing the core-degraded CSBM3 microgel with PBS buffer of pH = 8 containing various amount of glucose. As shown in Figure 8, the final absorbance of the mixture
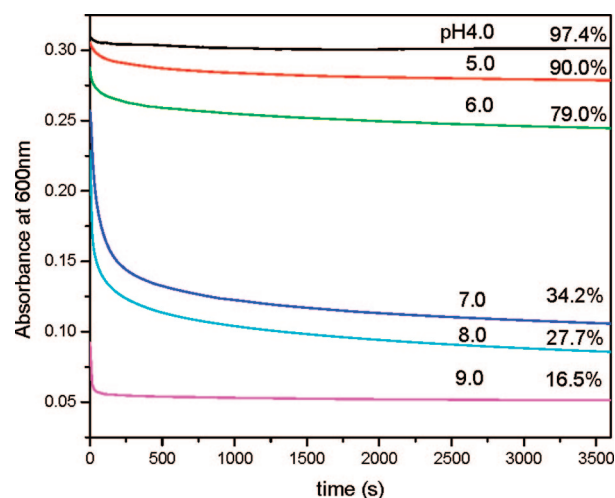
Figure 7. Release profiles of the degraded core polymer debris from CSBM 3 microgel in 0.005 M PBS of various pH values at 28 °C
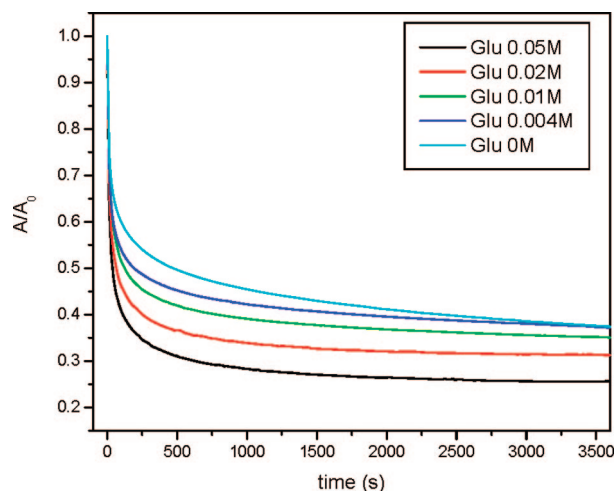
Figure 8. Release profiles of the degraded core polymer debris from CSBM3 microgels in 0.005 M PBS of pH = 8 in the presence of glucose at different concentrations.

decreases with the increase in glucose concentration, clearly verifying that the shell permeability increases with increasing glucose concentration. The result implies that if insulin is loaded in the core area, its release rate will increase with increasing glucose concentration in the media. This type of novel structured microgels may find applications for the self-regulated insulin delivery.

Conclusions

In conclusion, a core–shell microgel with a degradable DHEA-cross-linked PNIPAM core and a nondegradable BIS-cross-linked P(NIPAM-PBA) glucose-responsive shell can be synthesized. The PNIPAM core can be degraded with the addition of $NaIO_4$. At room temperature, the degraded polymer segments can be held by the collapsed P(NIPAM-PBA) shell. Temperature and pH change can control the permeability of the shell. A decrease in temperature or an increase in pH can both enhance the permeability of the shell. In addition, the shell permeability can be further tuned by glucose concentration. The increase in glucose concentration increases the shell permeability. The fundamental understanding of the permeability control of the glucose-responsive gel nanoshell is very important for the potential application of the PBA-conjugated microgels for self-regulated insulin delivery.

References and Notes

(1) Pelton, R. *Adv. Colloid Interface Sci.* **2000**, *85*, 1.
(2) Senff, H.; Richtering, W. *J. Chem. Phys.* **1999**, *111*, 1705.
(3) Das, M.; Zhang, H.; Kumacheva, E. *Annu. Rev. Mater. Res.* **2006**, *36*, 117.
(4) Bailey, R. C.; Nam, J.-M.; Mirkin, C. A.; Hupp, J. T. *J. Am. Chem. Soc.* **2003**, *125*, 13541.
(5) Bromberg, L.; Temchenko, M.; Hatton, T. A. *Langmuir* **2003**, *19*, 8675.
(6) Antonietti, M.; Grohn, F.; Hartmann, J.; Bronstein, L. *Angew. Chem., Int. Ed.* **1997**, *36*, 2080.
(7) Zhang, J.; Xu, S.; Kumacheva, E. *J. Am. Chem. Soc.* **2004**, *126*, 7908.
(8) Lyon, L. A.; Debord, J. D.; Debord, S. B.; Jones, C. D.; McGrath, J. G.; Serpe, M. J. *J. Phys. Chem. B* **2004**, *108*, 19099.
(9) Gao, J.; Hu, Z. *Langmuir* **2002**, *18*, 1360.
(10) Vinogradov, S. V. *Curr. Pharm. Des.* **2006**, *12*, 4703.
(11) Soppimath, K. S.; Tan, D. C.-W.; Yang, Y.-Y. *Adv. Mater.* **2005**, *17*, 318.
(12) Serpe, M. J.; Yarmey, K. A.; Nolan, C. M.; Lyon, L. A. *Biomacromolecules* **2005**, *6*, 408.
(13) Nayak, S.; Lee, H.; Chmielewski, J.; Lyon, L. A. *J. Am. Chem. Soc.* **2004**, *126*, 10258.
(14) Zhang, H.; Mardyani, S.; Chan, W. C. W.; Kumacheva, E. *Biomacromolecules* **2006**, *7*, 1568.
(15) Kraft, M. L.; Moore, J. S. *Langmuir* **2003**, *19*, 910.
(16) Nayak, S.; Lyon, L. A. *Angew. Chem., Int. Ed.* **2004**, *43*, 6706.
(17) Zhang, Y.; Guan, Y.; Zhou, S. *Biomacromolecules* **2006**, *7*, 3196.
(18) Lapeyre, V.; Gosse, I.; Cheviane, C.; Ravaine, V. *Biomacromolecules* **2006**, *7*, 3356.
(19) Ge, H.; Ding, Y.; Ma, C.; Zhang, G. *J. Phys. Chem. B* **2006**, *110*, 20635.
(20) Hoare, T.; Pelton, R. *Macromolecules* **2007**, *40*, 670.
(21) Chu, B. *Laser Light Scattering*, 2nd ed.; Academic Press: New York, 1991.
(22) Stockmayer, W. H.; Schmidt, M. *Pure Appl. Chem.* **1982**, *54*, 407.
(23) Jones, C. D.; Lyon, L. A. *Macromolecules* **2000**, *33*, 8301.
(24) Jones, C. D.; Lyon, L. A. *Macromolecules* **2003**, *36*, 1988.
(25) Jones, C. D.; Lyon, L. A. *Langmuir* **2003**, *19*, 4544.
(26) Berndt, I.; Richtering, W. *Macromolecules* **2003**, *36*, 8780.
(27) Chen, Y.; Gautrot, J. E.; Zhu, X. X. *Langmuir* **2007**, *23*, 1047.
(28) O'Connell, P. B. H.; Brady, C. J. *Anal. Biochem.* **1976**, *76*, 63.
(29) Nayak, S.; Gan, D.; Serpe, M. J.; Lyon, L. A. *Small* **2005**, *1*, 416.
(30) Matsumoto, A.; Yoshida, R.; Kataoka, K. *Biomacromolecules* **2004**, *5*, 1038.